CrIS Noise and Calibration Uncertainty

David Tobin, Joe Taylor, Lori Borg, Michelle Feltz, Dan Deslover, Bob Knuteson, Hank Revercomb
CIMSS/SSEC, UW-Madison

The 22nd International TOVS Study Conference (ITSC-22)
Saint-Sauveur, Canada

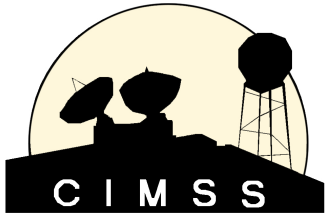

CrIS Operational Concept

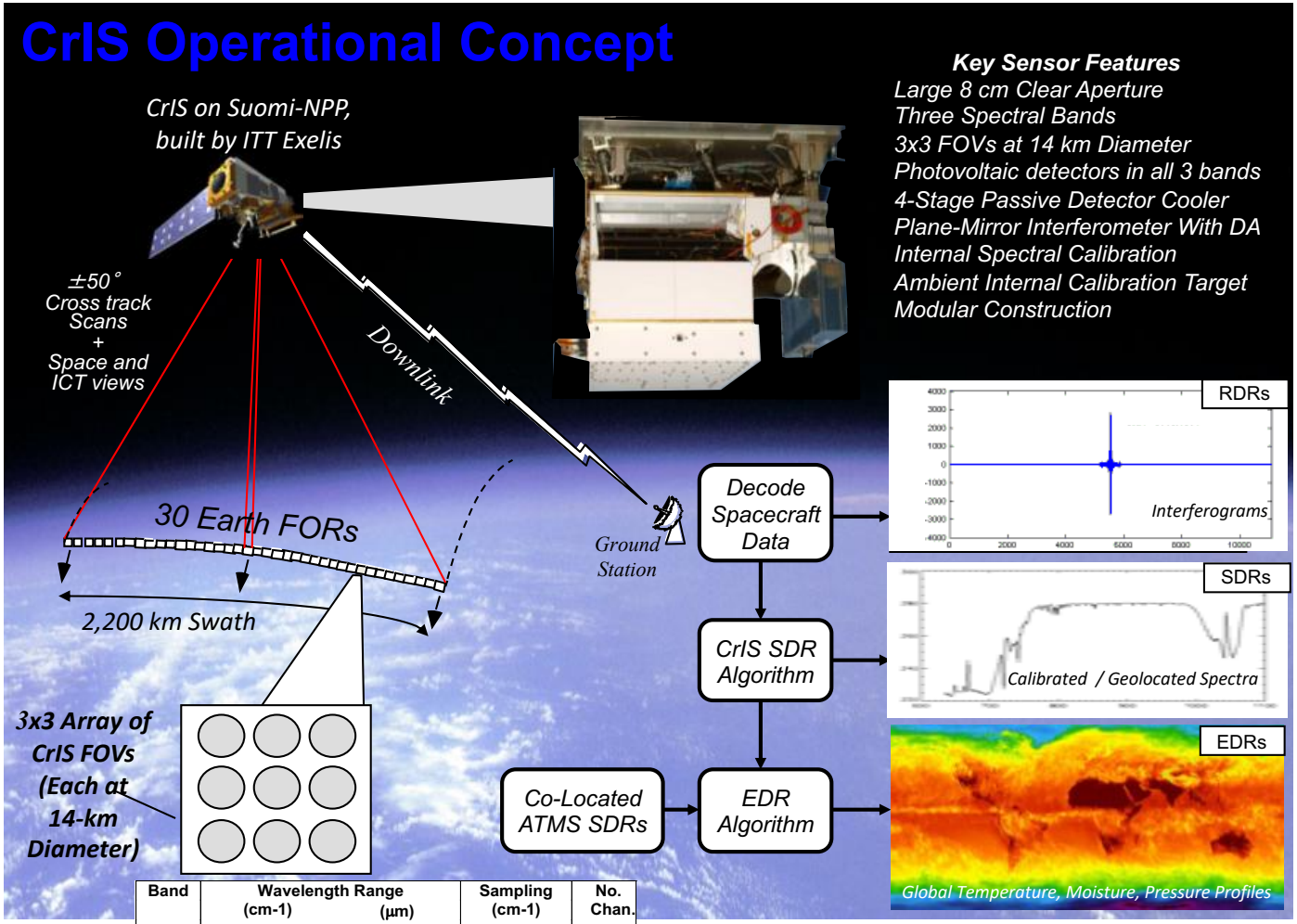

Key Sensor Features

Large 8 cm Clear Aperture
Three Spectral Bands
3x3 FOVs at 14 km Diameter
Photovoltaic detectors in all 3 bands
4-Stage Passive Detector Cooler
Plane-Mirror Interferometer With DA
Internal Spectral Calibration
Ambient Internal Calibration Target
Modular Construction

Band	Wavelength Range (cm-1)	(μm)	Sampling (cm-1)	No. Chan.
SWIR	2155-2550	4.64-3.92	2.5	159
MWIR	1210-1750	8.26-5.71	1.25	433
LWIR	650-1095	15.38-9.14	0.625	713

Example Longwave Spectra

Monochromatic

AIRS

(near Gaussian SRFs)

Monochromatic

IASI L1C

(+/-2cm OPD w/ Gaussian apodization)

Monochromatic

CrIS unapodized

(+/-0.8 cm OPD, SDRs)

Monochromatic

CrIS with Hamming apodization

($R'_i = 0.23\ R_{i-1} + 0.54\ R_i + 0.23\ R_{i+1}$, BUFR)

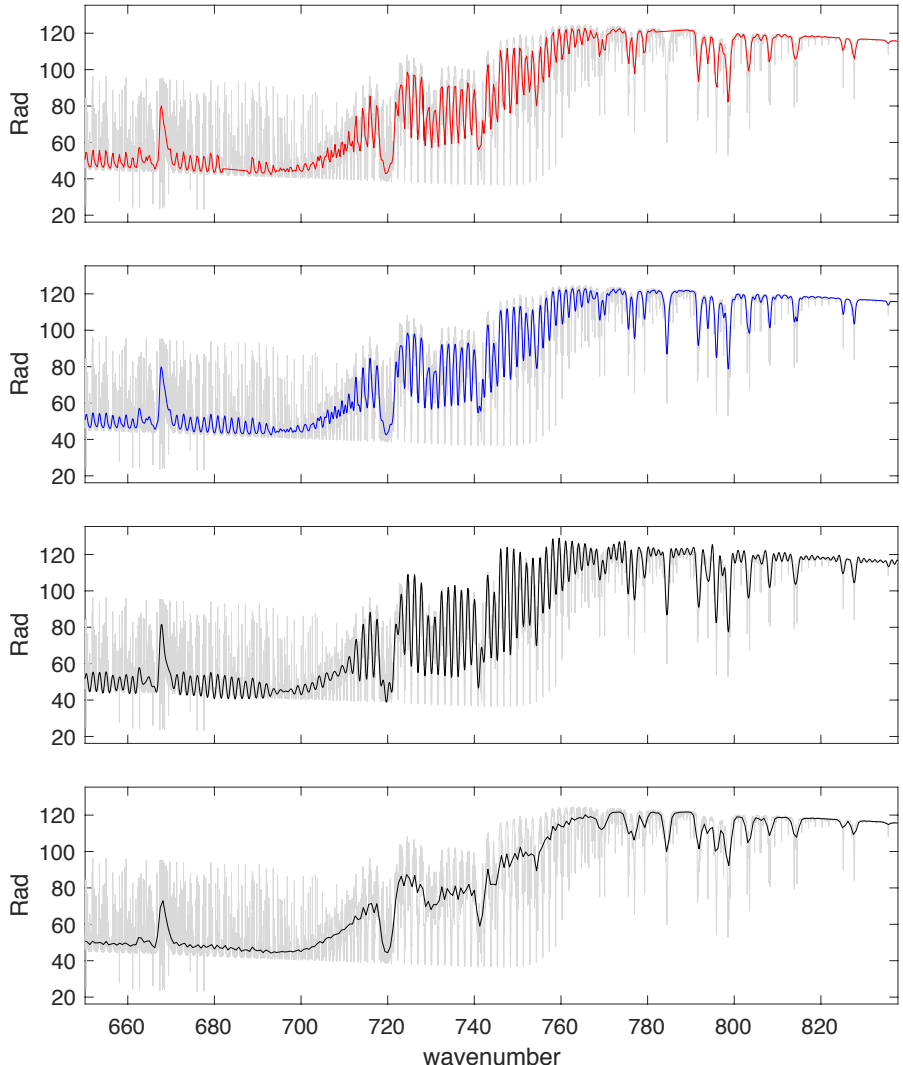

Example hyperspectral IR Clear sky Covariance

from Bormann et al., “Enhancing the impact of IASI observations through an updated observation-error covariance matrix”

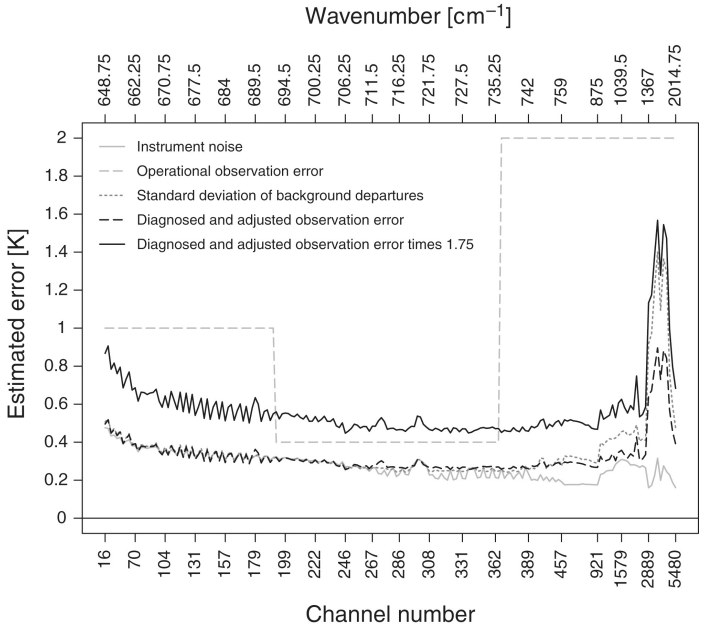

Observation-error correlations for assimilated IASI channels:

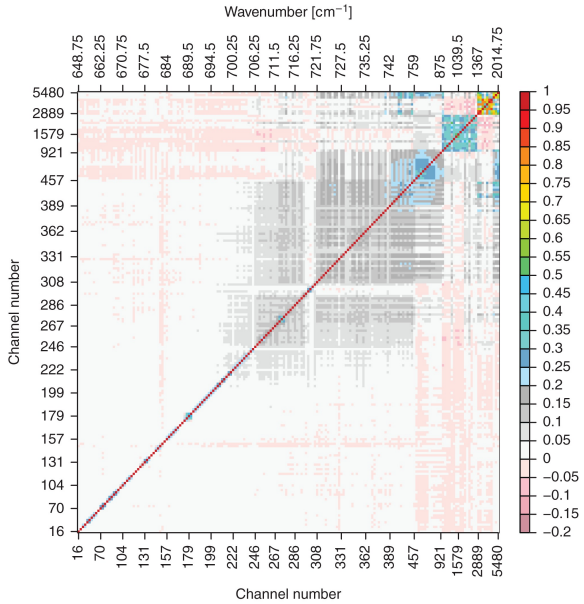

“Observation Error” contributors:

- Instrument Noise
- Instrument Calibration uncertainties
- Forward Model error (Fast model and underlying LBL)
- Representativeness Error
- Cloud contamination
- Quality Control errors
- …

Error standard deviations:

- Close to instrument noise for upper tropospheric and stratospheric temperature sounding channels, with weak error correlations;
- Larger than the instrument noise for water-vapour channels, combined with significant interchannel error correlations; and
- Larger than the instrument noise for lower temperature sounding, window and ozone channels, together with weaker, but still significant, interchannel error correlations.

Outline

- CrIS instrument noise
  - Gaussian distribution
  - Scene independence of NEDN
  - FOV variability
  - Spectral correlation
  - Self-apodization correction and Hamming apodization effects on NEDN level and spectral correlation
- CrIS Calibration uncertainties
  - Contributors
  - Warm and cold scene examples
- Next steps

Calibrated ICT (onboard blackbody) spectra ensembles

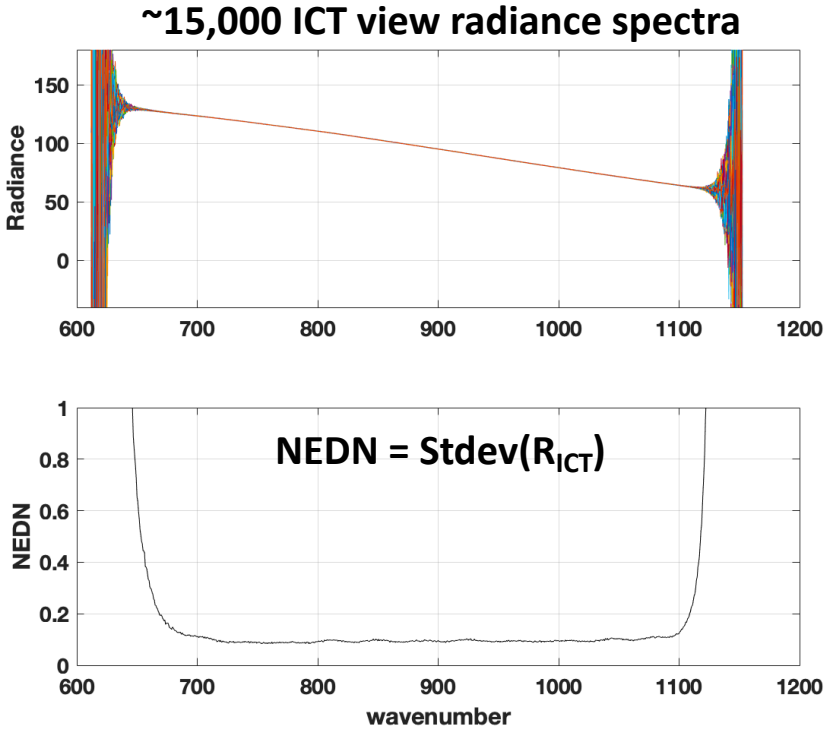

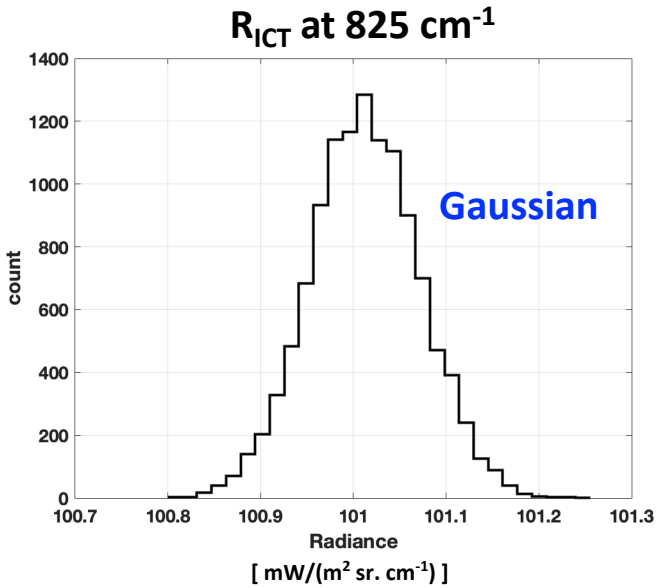

NEDN vs NEDT

NOAA20 measured NEDN for 200K scene:

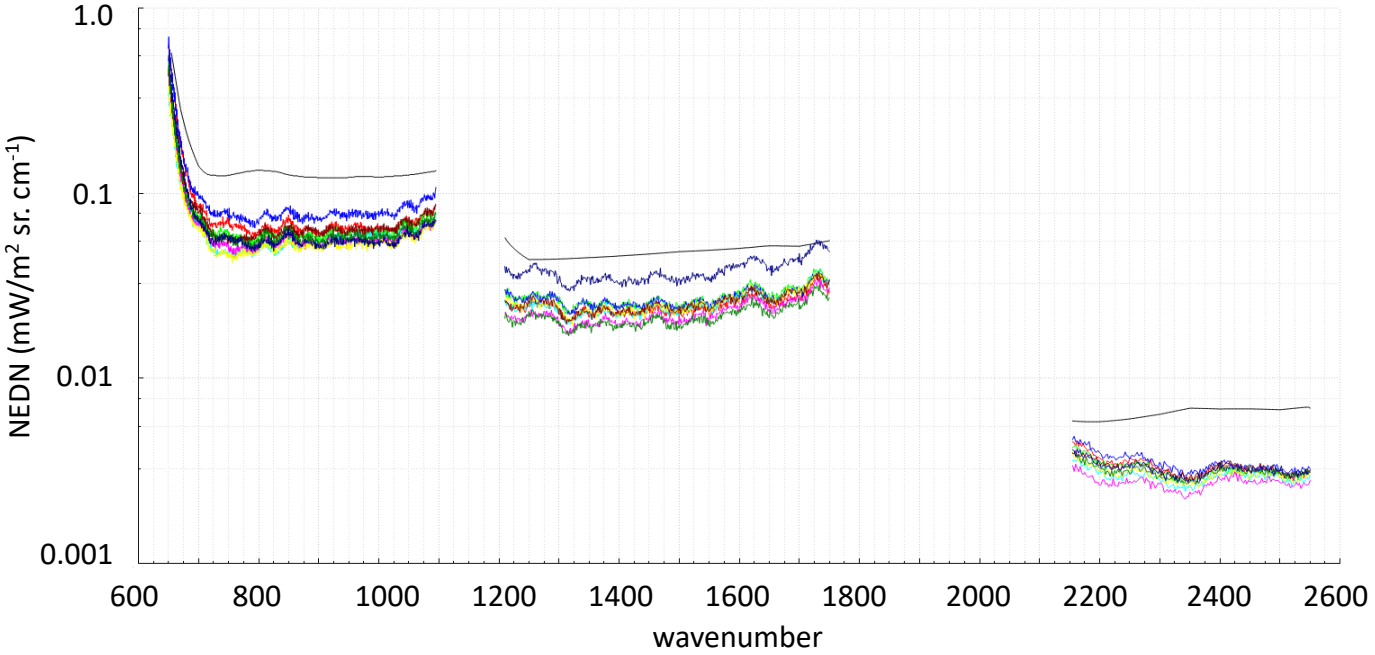

NEDN vs NEDT

NOAA20 measured NEDN for 233K scene:

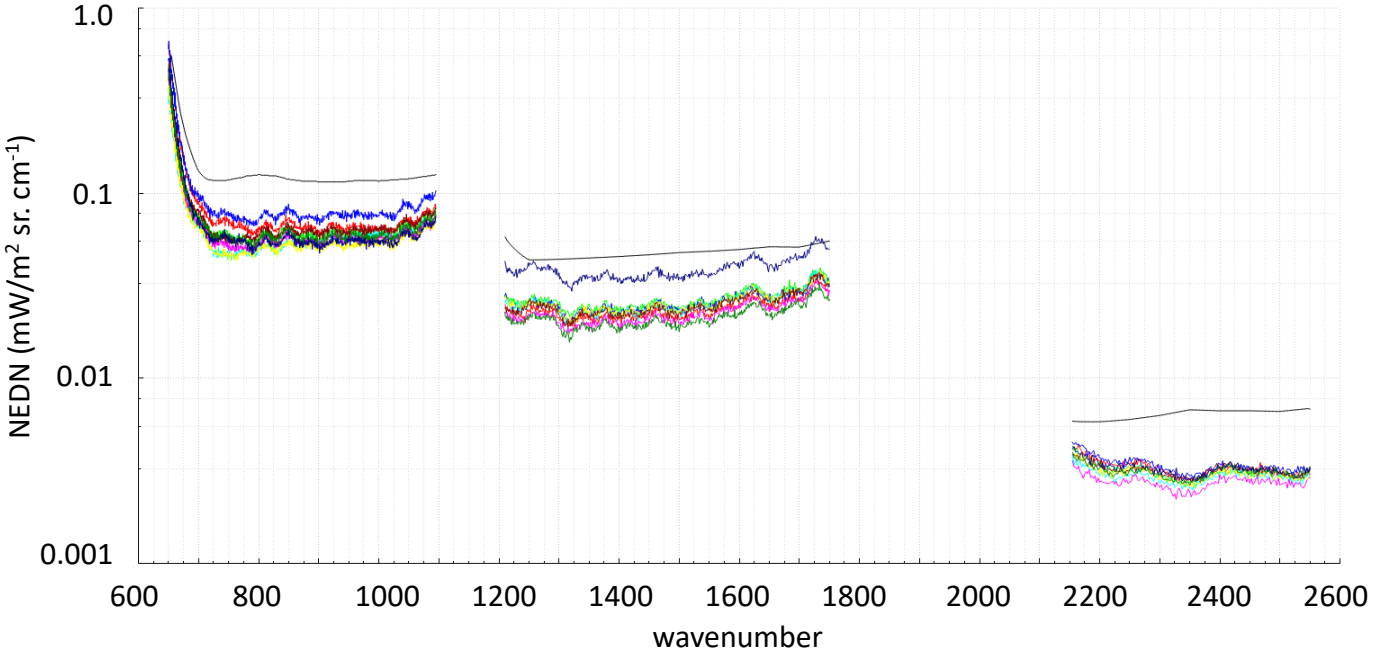

NEDN vs NEDT

NOAA20 measured NEDN for 260K scene:

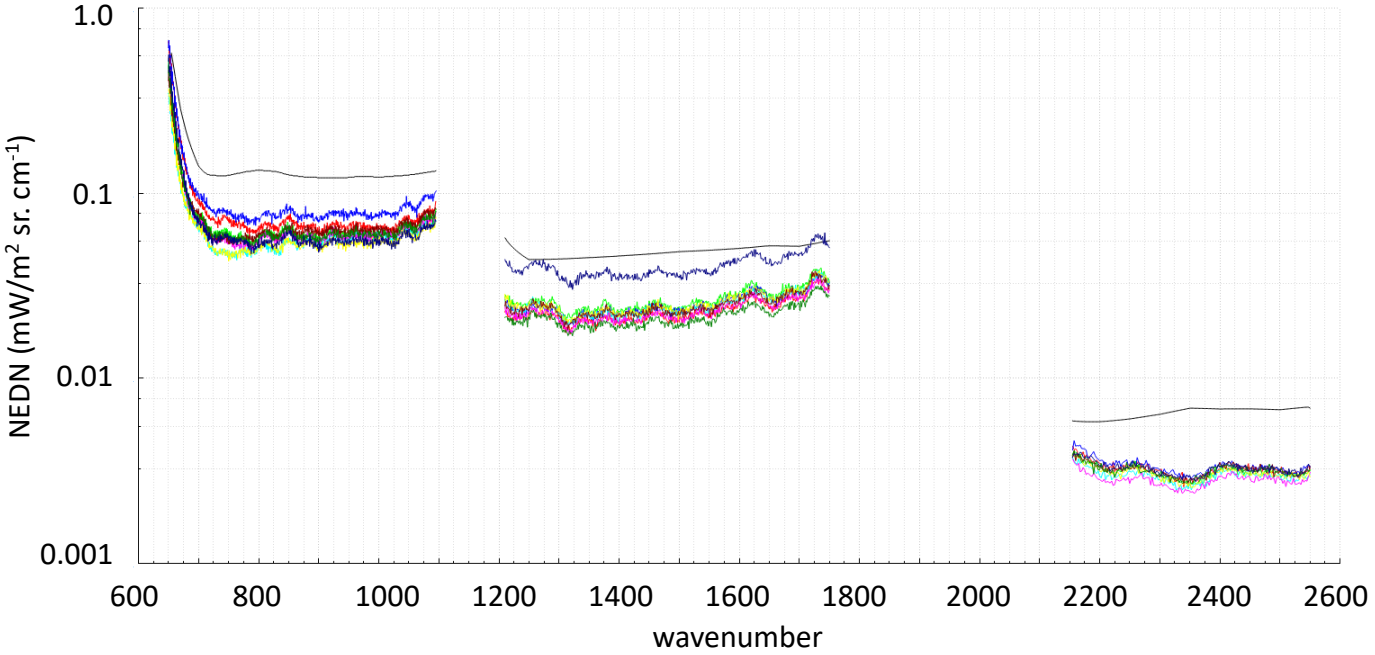

NEDN vs NEDT

NOAA20 measured NEDN for 287K scene:

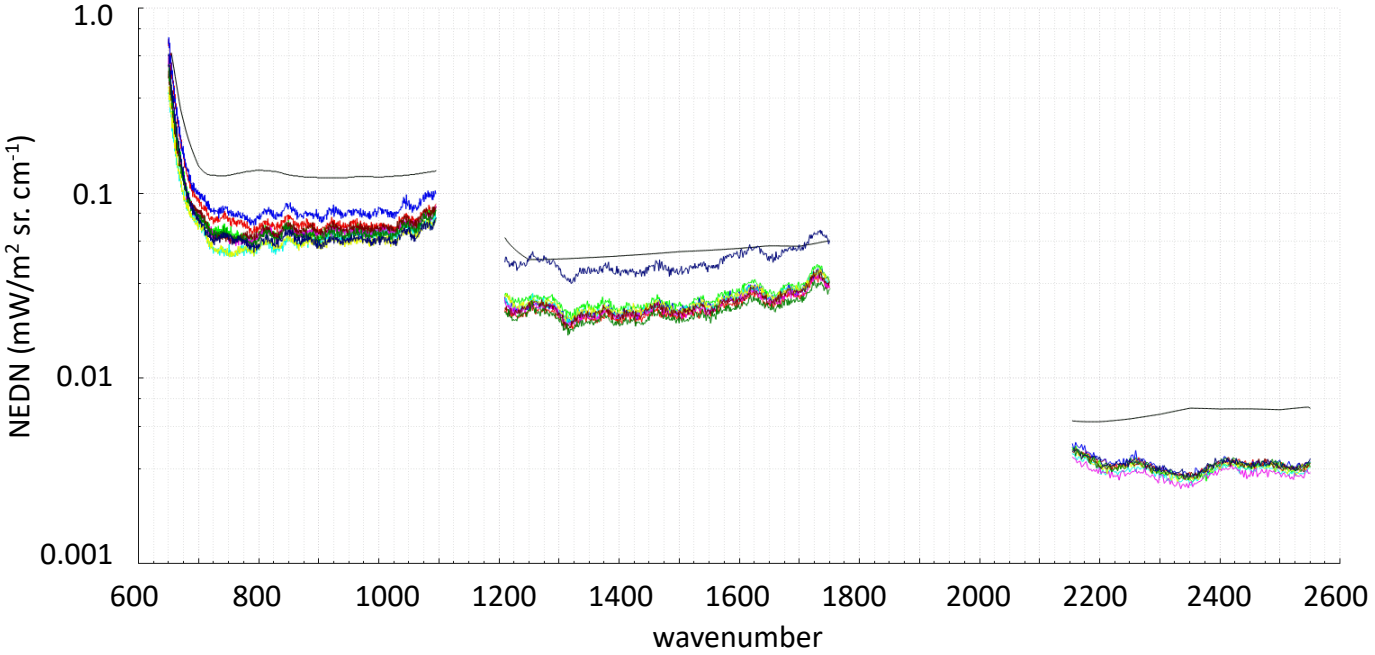

NEDN vs NEDT

NOAA20 measured NEDN for 299K scene:

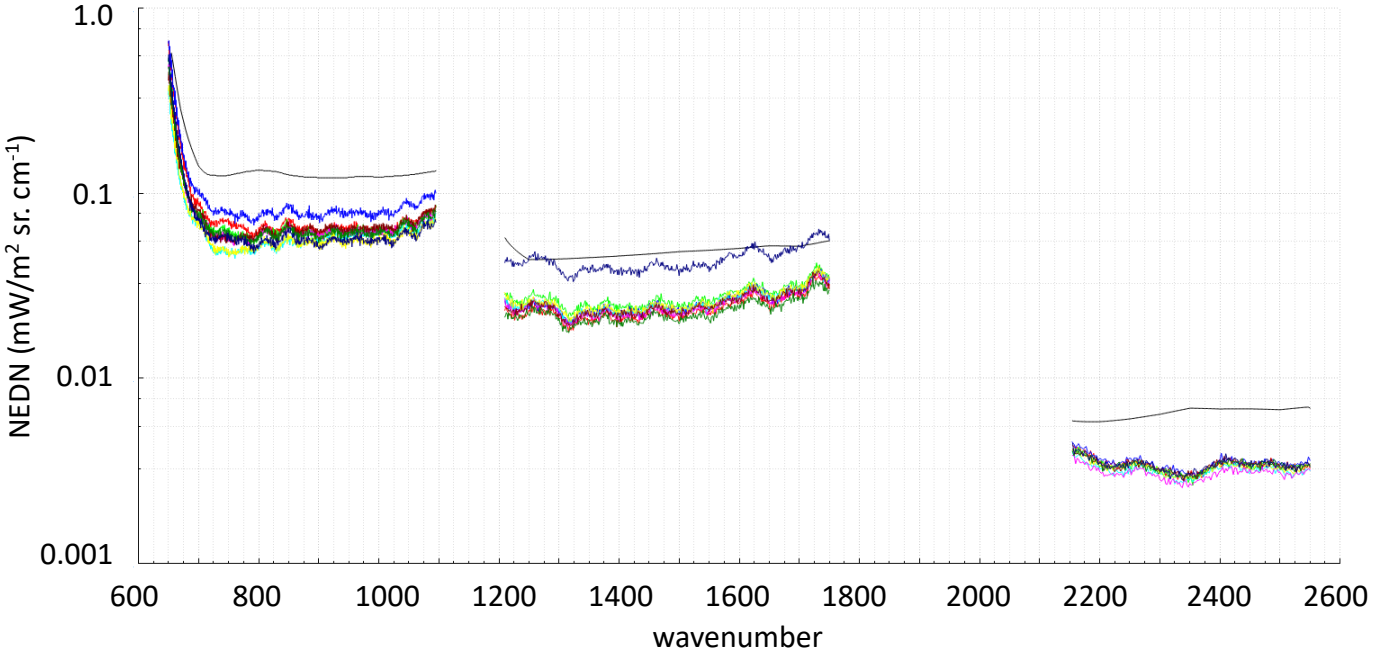

NEDN vs NEDT

NOAA20 measured NEDN for 310K scene:

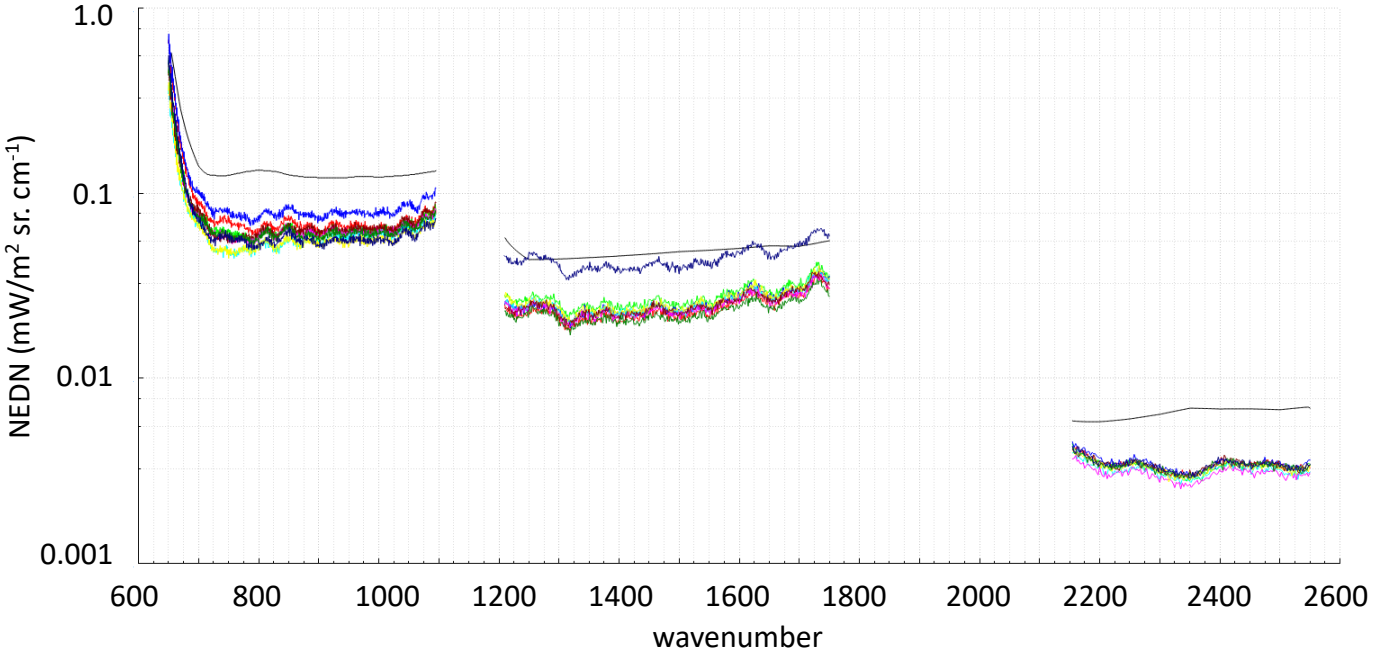

NEDN converted to NEDT at various scene temperatures

(NEDN [mW/(m^2 sr. cm^{-1})] = 0.1 LW; 0.04 MW; 0.006 SW)

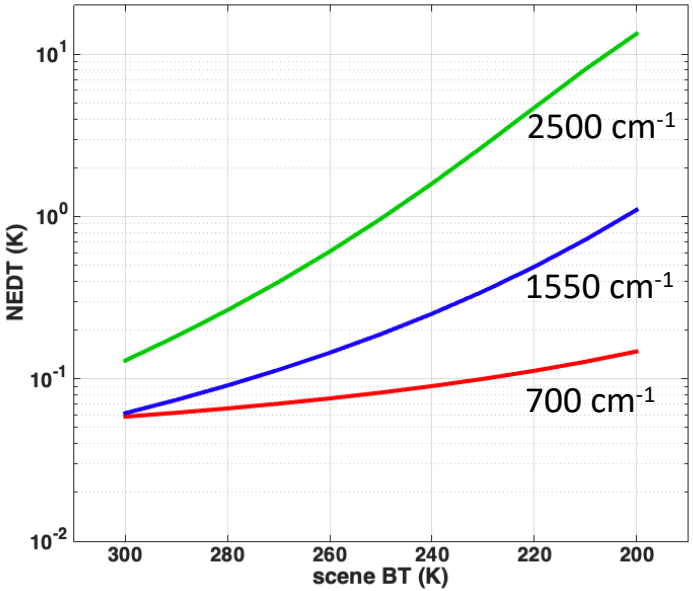

NEDN converted to NEDT at 280K and at scene temperature of a typical clear sky spectrum

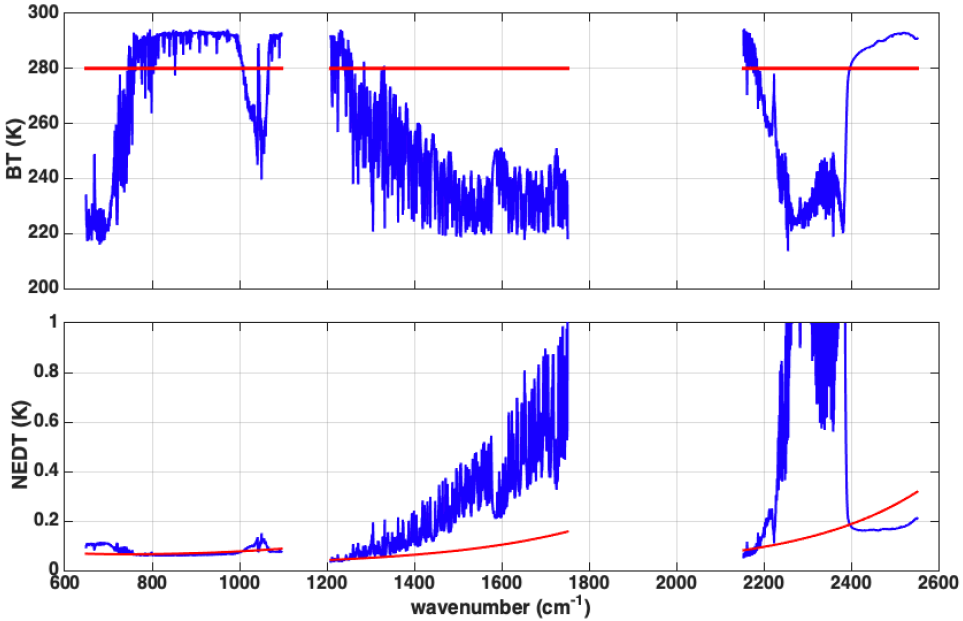

FOV variability of NEDN SNPP CrIS

- 30% variations in LW NEDN among FOVs
- In the MW, FOV7 is the large outlier, with NEDN ~3 times higher than other FOVs. (This detector also has the largest nonlinearity of the SNPP MW FOVs)
- MW and SW bands show self-apodization noise amplification, with values up to 70% (FOV3) greater than on-axis FOV5 at end of SW band

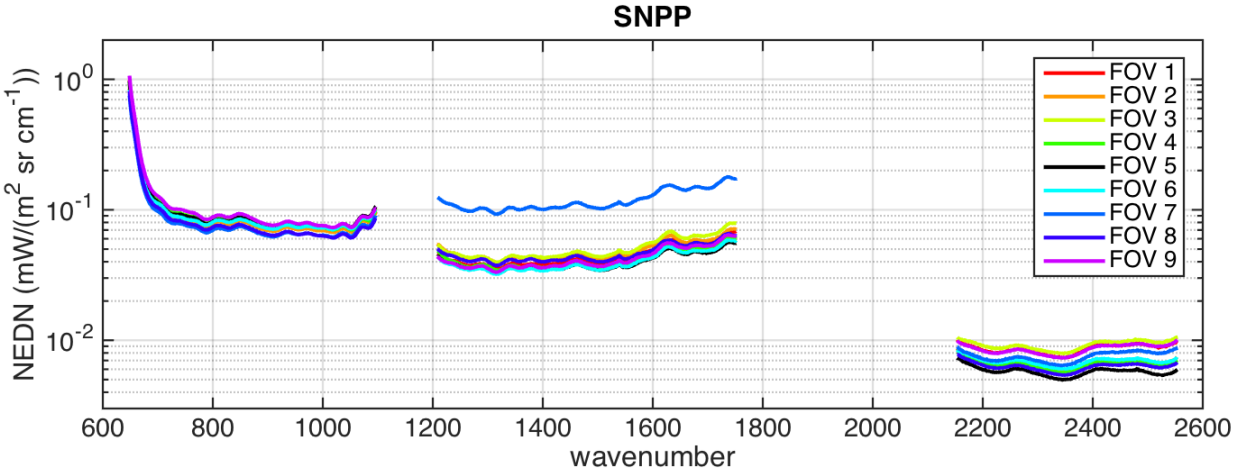

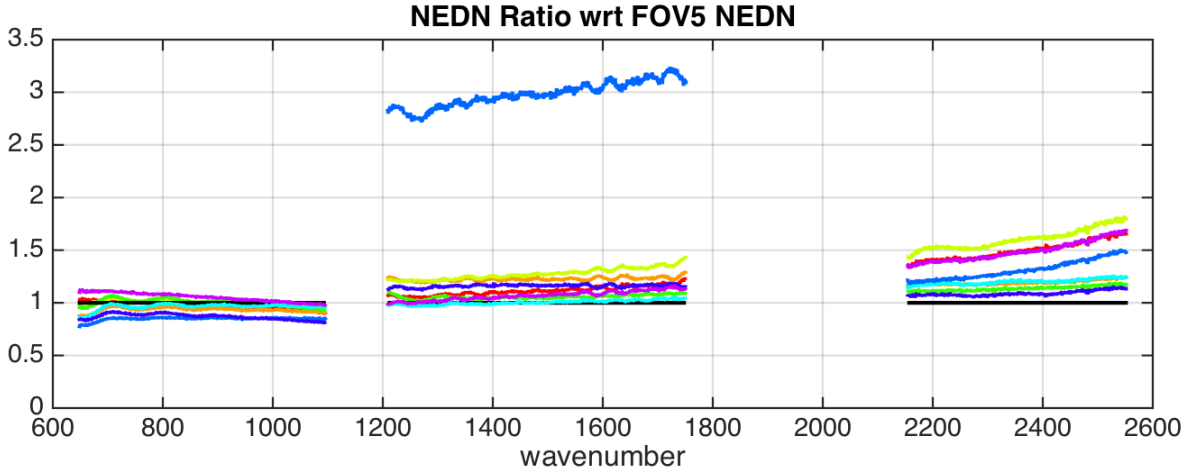

FOV variability of NEDN NOAA20 CrIS

- ~75% variation among FOVs in the LW band, with FOVs 7 and 4 as notable outliers
- In the MW, FOV9 has ~2x higher noise than other FOVs. (It also has nigh nonlinearity (the other NOAA20 MW FOVs are ~linear) and is from the same detector lot as SNPP FOV7.) Aside from FOV9, MW variations are ~15%.
- SW variations are similar to SNPP.

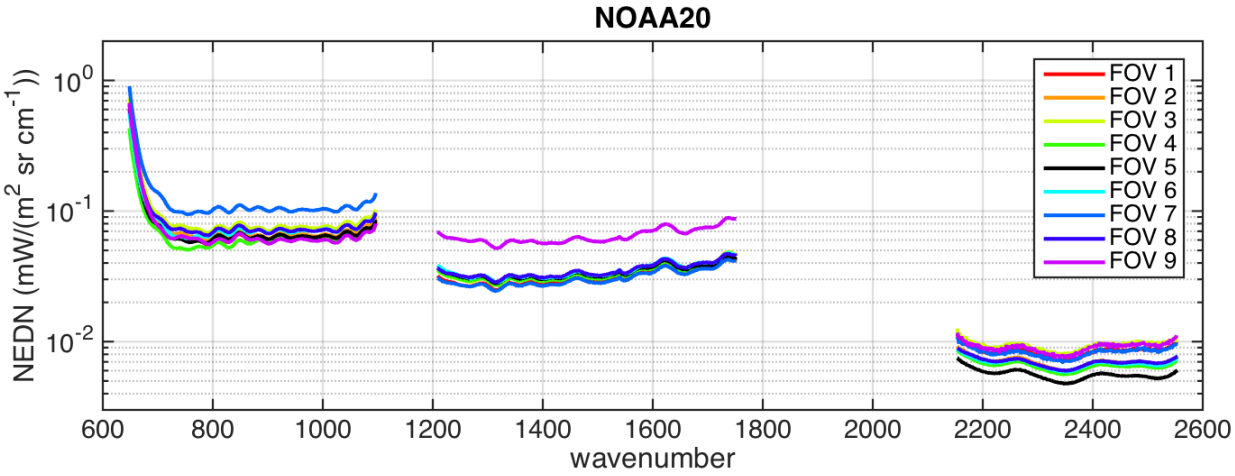

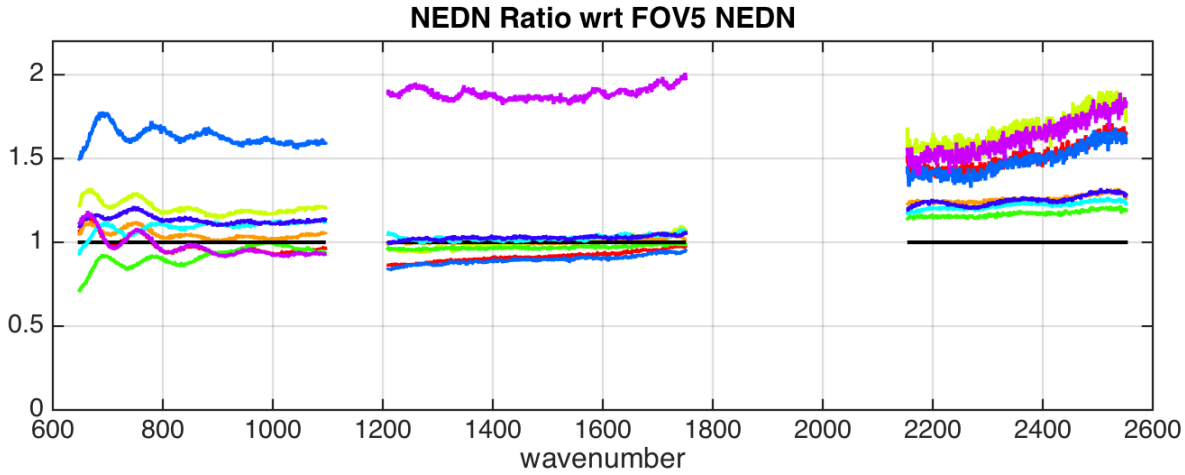

SNPP spectrally correlated noise, Pre-launch testing

Midwave band FOV5 example from Zavyalov et al., Noise performance of the CrIS instrument

Baseline environment

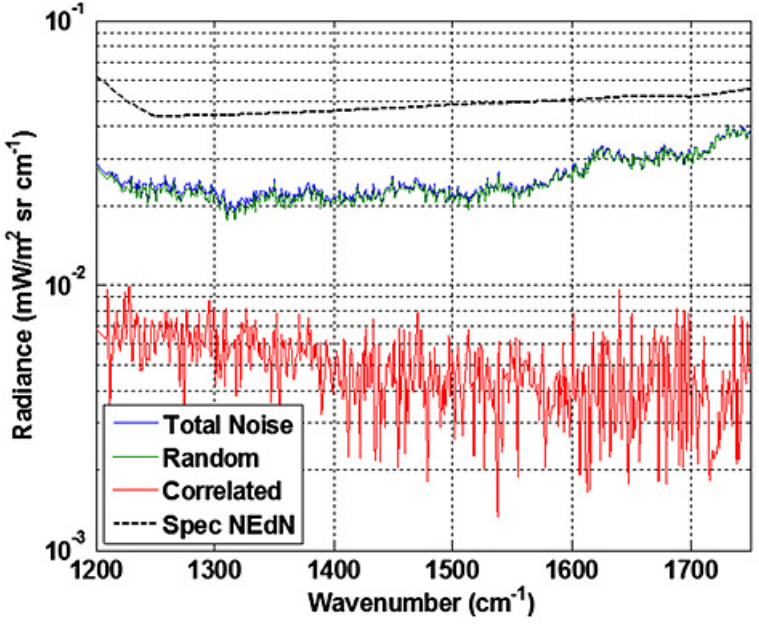

With external vibration

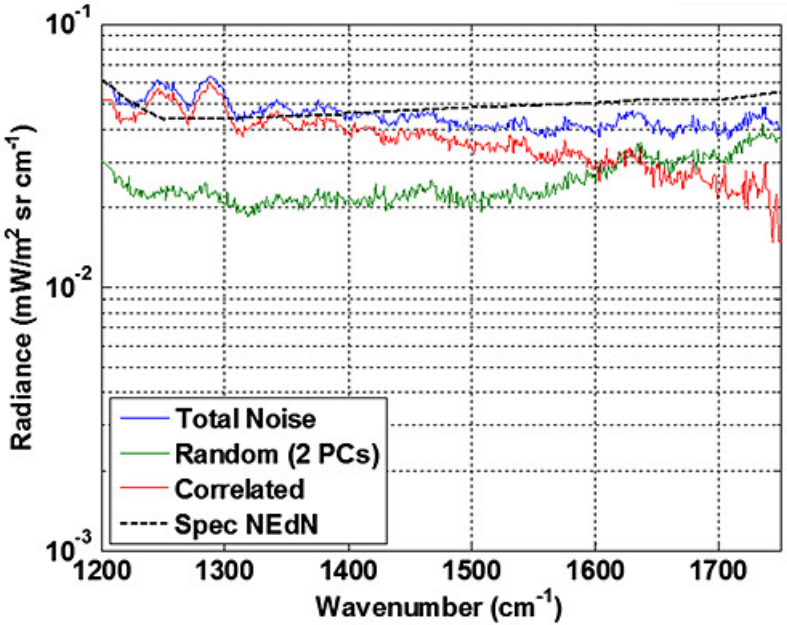

Journal of Geophysical Research: Atmospheres, Volume: 118, Issue: 23, Pages: 13,108-13,120, First published: 25 November 2013, DOI: (10.1002/2013JD020457)

Correlated (red) and random noise (green) contribution to the total NEdN (blue) estimated from the ECT spectra acquired during dynamic interaction test for center FOV5 in MWIR spectral band. (a) Baseline NEdN is compared with (b) NEdN estimated for an external vibration of 5·10−3 g0 injected along the Y axis at 158 Hz. Black line is a spec NEdN value.

SNPP spectrally correlated noise

Shortwave band example from Zavyalov et al., Noise performance of the CrIS instrument

Random/correlated noise contribution to the total NEdN in SWIR spectral band estimated for all nine FOVs from the ICT data acquired on 10 January 2013, Orbit 6245. Note that the blue line (total noise) overlays the green line (random noise).

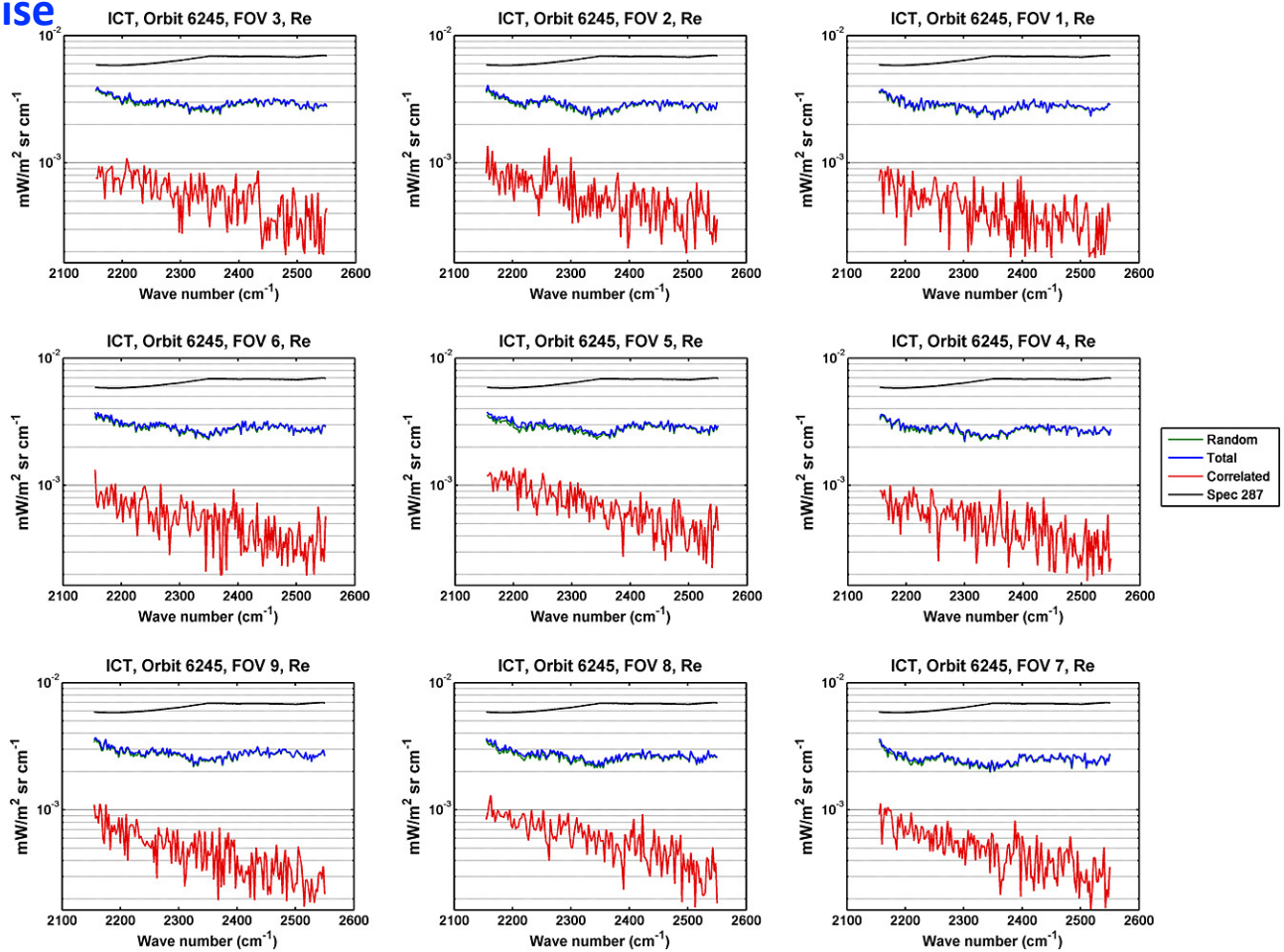

Examples for EOS-Aqua Atmospheric InfraRed Sounder

NEDN versus scene radiance

NEDN increases with sqrt{scene radiance}, consistent with photon noise. The total noise at scene temperature T is parameterized as

$$NEDN(T) = [N(T)\,\gamma_{photon} + NEDN_{thermal}^2]^{1/2}$$

where $NEDN_{thermal}^2$ (the y-intercepts) and γ_{photon} (the slopes) are determined for each channel.

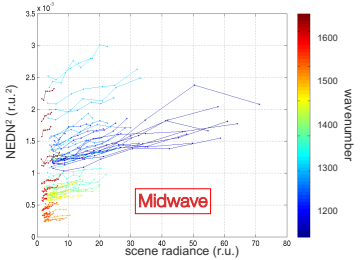

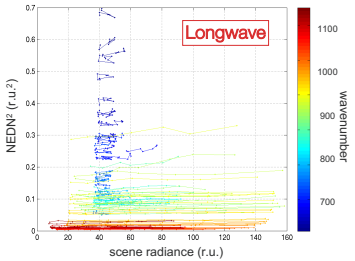

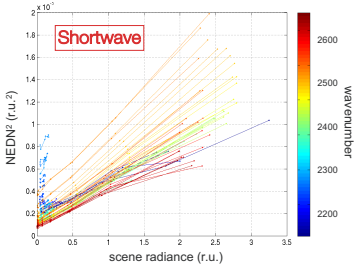

Spectrally Correlated Noise

The PCA estimate is of the spectrally uncorrelated noise; the spectrally correlated noise is computed as [total_noise^2 - pca_noise^2]$^{1/2}$ and compared to pre-flight determinations performed by JPL/BAE:

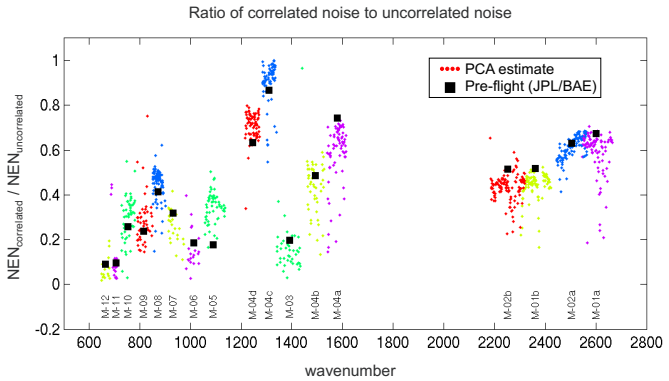

- Very good agreement between two very different and independent analyses.
- The correlated noise is a large fraction of the total noise for several arrays.

Suomi-NPP CrIS Observed and Calculated Instrument Lineshapes FOVs 5, 4, and 1

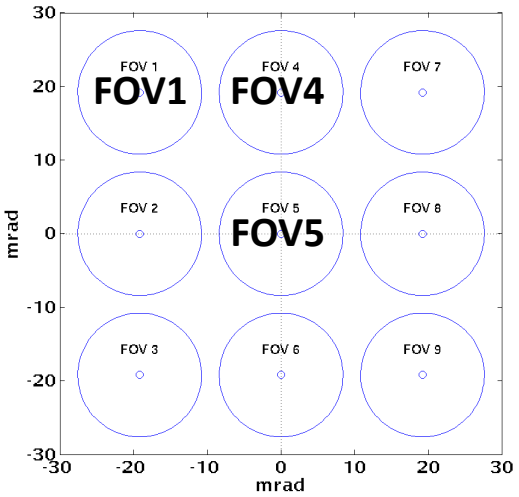

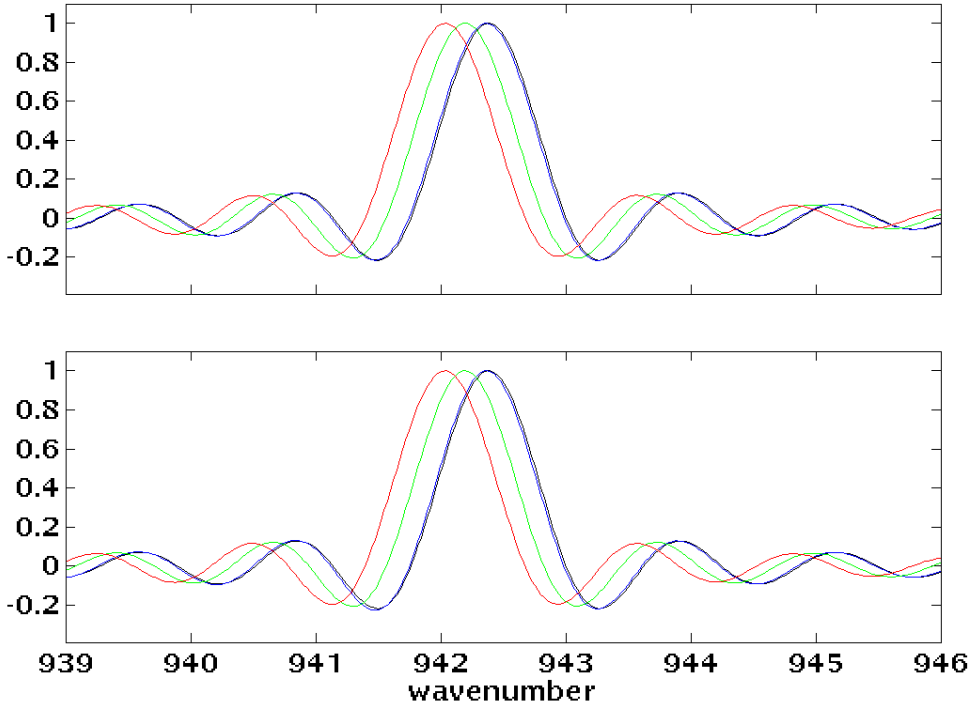

CrIS Calibration Equation/Algorithm

$$\tilde{L}^{es} = L^{ict} \cdot \frac{F \cdot f_{ATBD} \cdot SA_s^{-1} \cdot f_{ATBD} \cdot \left[\frac{\Delta S_1}{\Delta S_2} \middle| \Delta S_2 \middle| \right]}{F \cdot f_{ATBD} \cdot SA_s^{-1} \cdot f_{ATBD} \cdot \left| \Delta S_2 \right|}$$

$\Delta S_1 = S_{ES} - S_{DS}$ $\Delta S_2 = S_{ICT} - S_{DS}$

- Complex calibration method (Revercomb, 1988) used for radiometric calibration
- Onboard neon source for spectral calibration
- Instrument self-apodization (*SA*) correction via inverse self apodization operator (Genest and Tremblay, 1999; Desbiens et al., 2006)

➢ **SA^{-1} is a de-apodization process, amplifying and correlating signal and noise**

- Han et al., "Effect of self-apodization correction on Cross-track Infrared Sounder radiance noise"

NEDN amplifications due to SA^{-1}

Han et al., “Effect of self-apodization correction on Cross-track Infrared Sounder radiance noise”

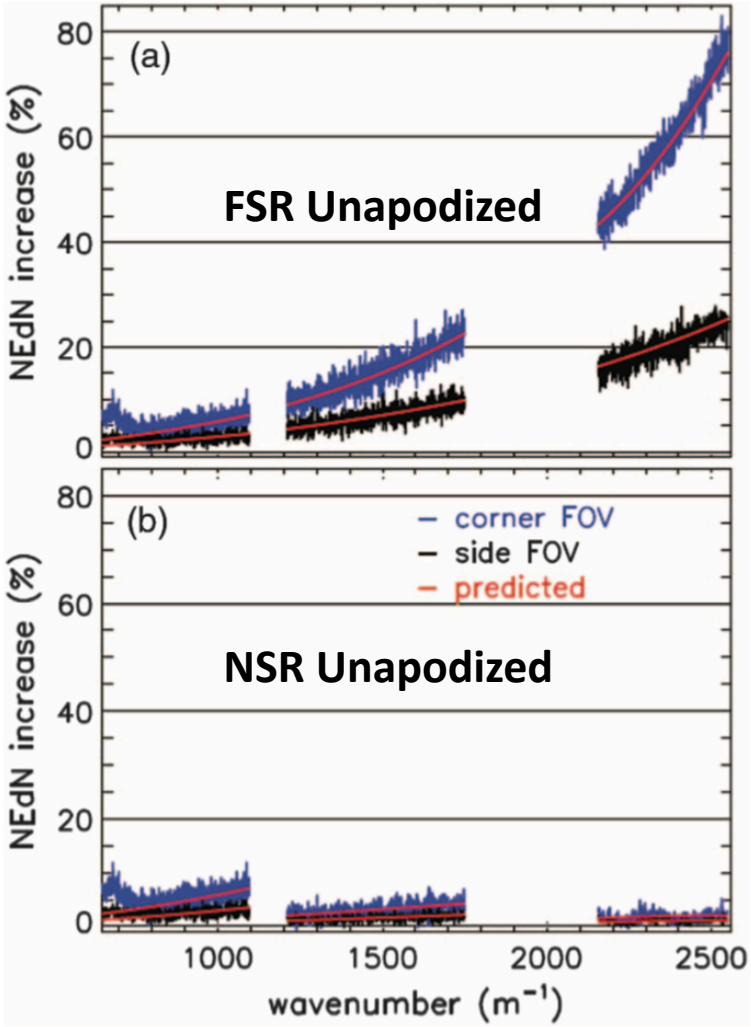

CrIS Noise Covariance example

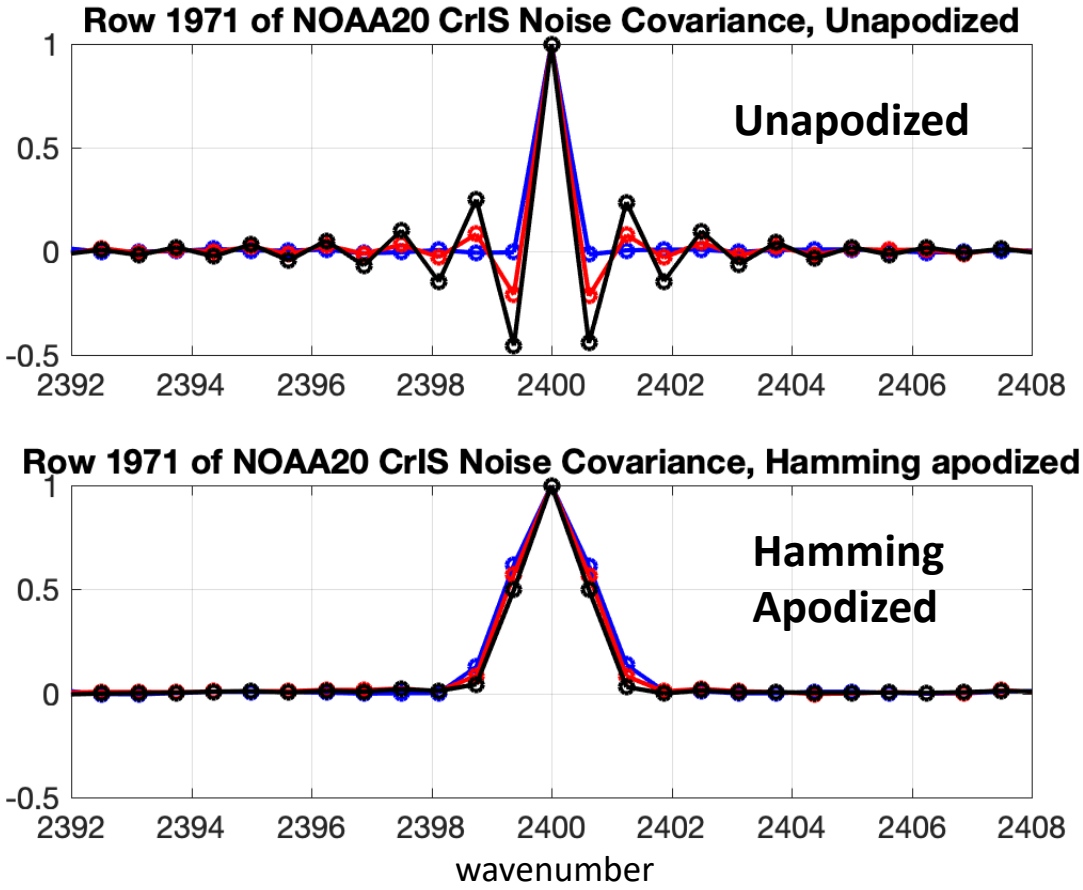

Center FOV
Side FOV
Corner FOV

CrIS Noise Covariance example

FOV1 noise covariance, Hamming apodized, log scale

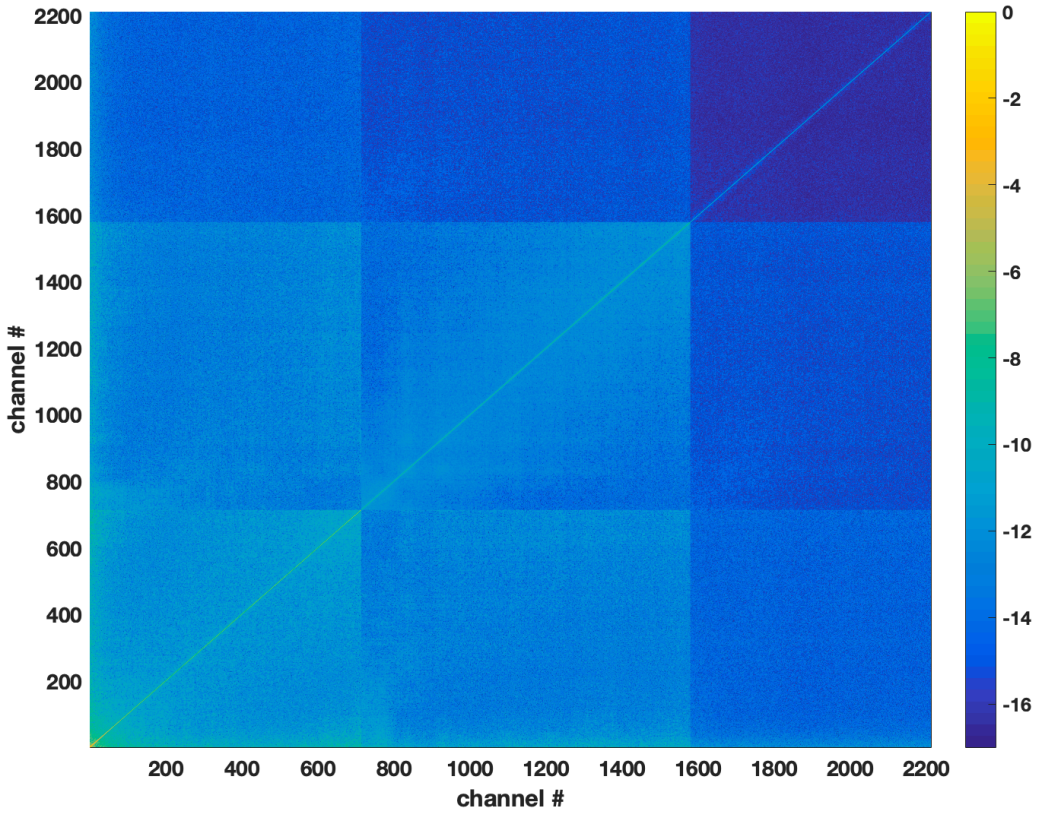

Effects of SA^{-1} and Hamming Apodization on NEDN

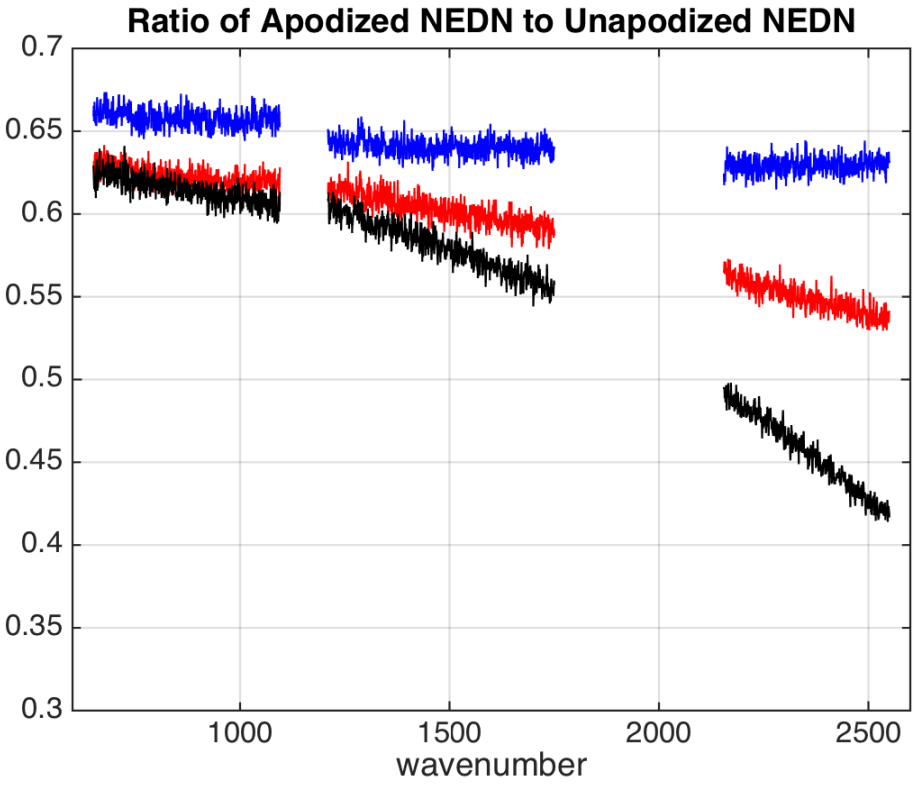

Center FOV
Side FOV
Corner FOV

Spectral correlation due to SA^{-1} and Hamming apodization

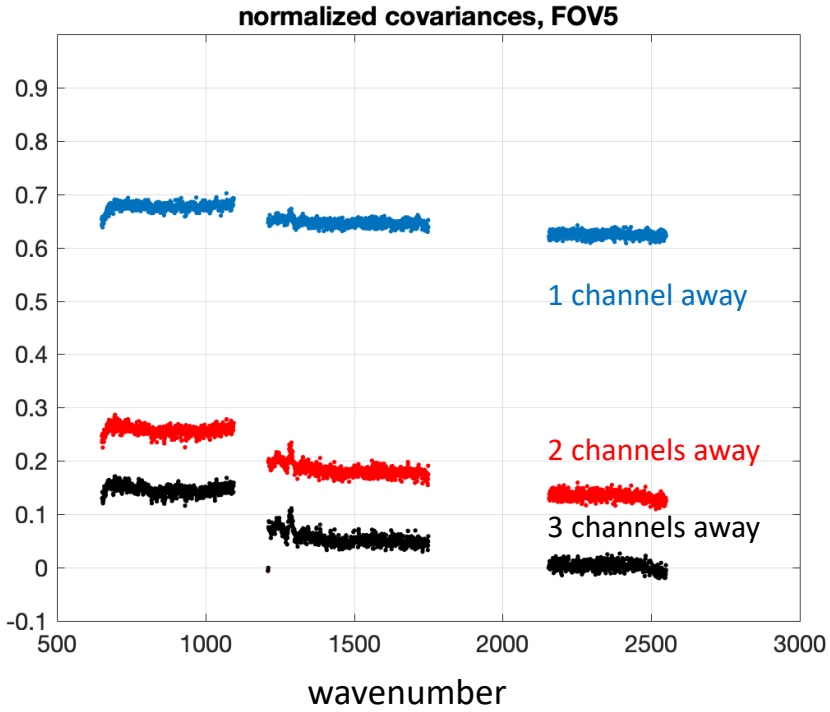

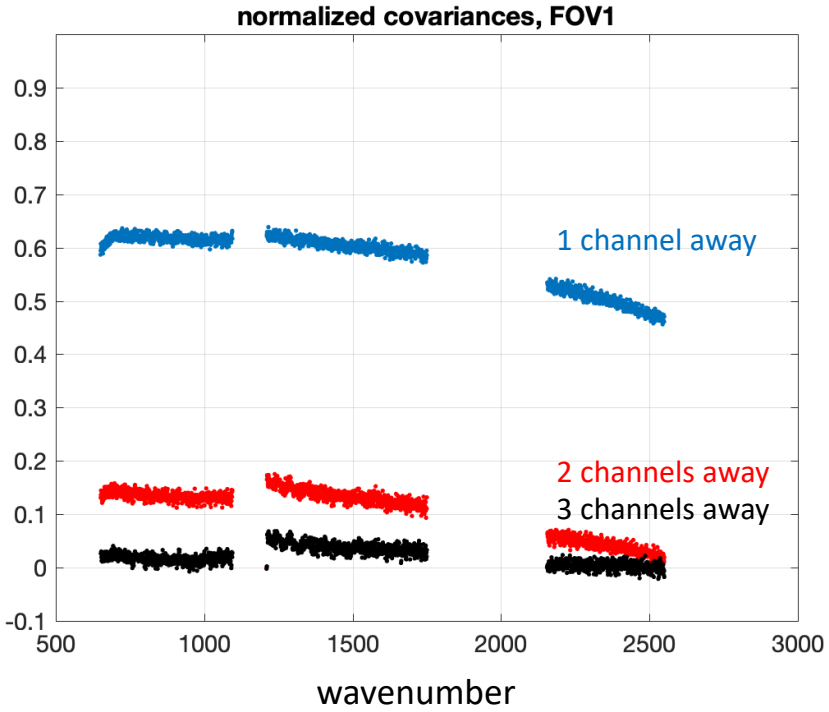

CrIS Simplified On-Orbit Radiometric Calibration Equation:

$$L_S = \mathbf{Re}\{(C'_{ES} - C'_{DS}) / (C'_{ICT} - C'_{DS})\}\ R_{ICT}$$

for observed complex spectra, C, of the Earth scene (**ES**), Internal Calibration Target (**ICT**), and Deep Space (**DS**) views.

with:

1. ICT Predicted Radiance: $R_{ICT} = \varepsilon_{ICT}\, B(T_{ICT}) + (1-\varepsilon_{ICT})\, B(T_{ICT,\,Refl})$

2. Quadratic Nonlinearity Correction: $C' = C \cdot (1 + 2\, a_2\, V_{DC})$

3. $$E_p \cong p_r p_t \left\{ \begin{array}{l} L_S \cos 2(\delta_S - \alpha) - L_H \dfrac{L_S - L_C}{L_H - L_C} \cos 2(\delta_H - \alpha) - L_C \dfrac{L_H - L_S}{L_H - L_C} \cos 2(\delta_C - \alpha) \\ -B_{SSM} \left[\cos 2(\delta_S - \alpha) - \dfrac{L_S - L_C}{L_H - L_C} \cos 2(\delta_H - \alpha) - \dfrac{L_H - L_S}{L_H - L_C} \cos 2(\delta_C - \alpha) \right] \end{array} \right\}$$

for polarization coefficients $p_r p_t$, scene selection mirror polarization angle δ, sensor polarizer angle α, and emission from the scene mirror B_{SSM}. *(H==ICT, C==DS).*

Example Radiometric Uncertainty estimates

For a warm clear sky scene (~worst case)

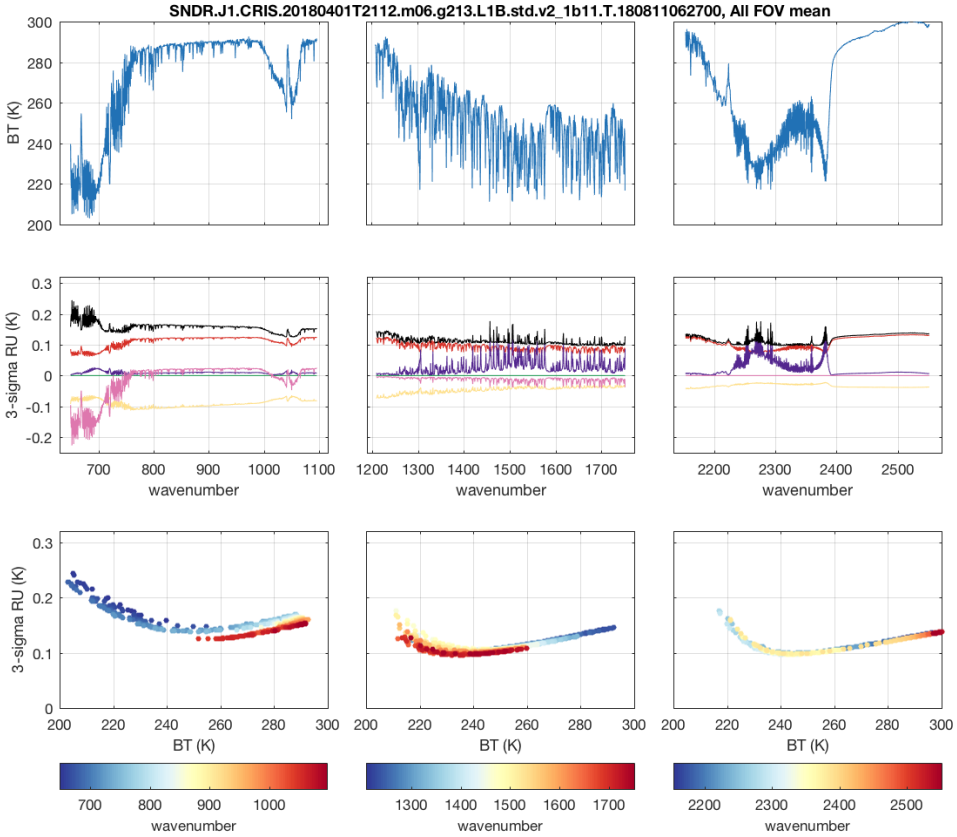

T_{ICT}
ε_{ICT}
$T_{refl,meas}$
$T_{refl,model}$
$p_r\, p_t$
a_2
Total

Example Radiometric Uncertainty estimates

For a cold cloud scene

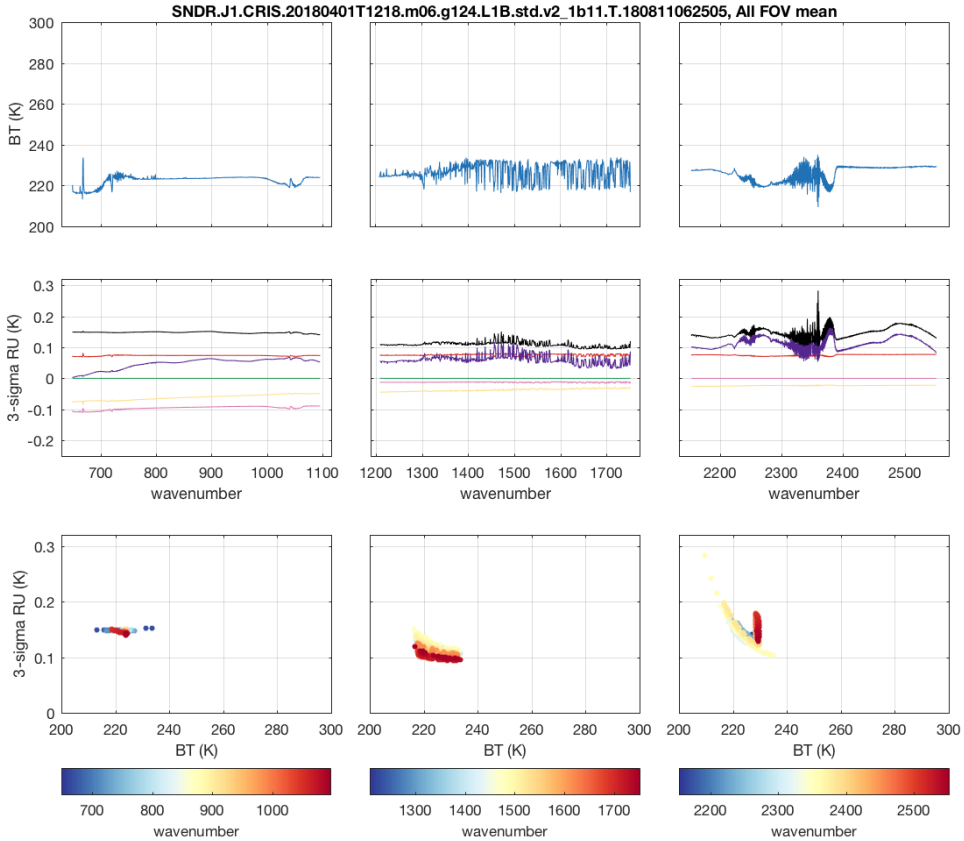

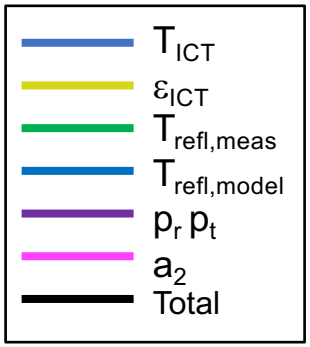

Calibration Uncertainty Covariance examples

Warm clear sky scene

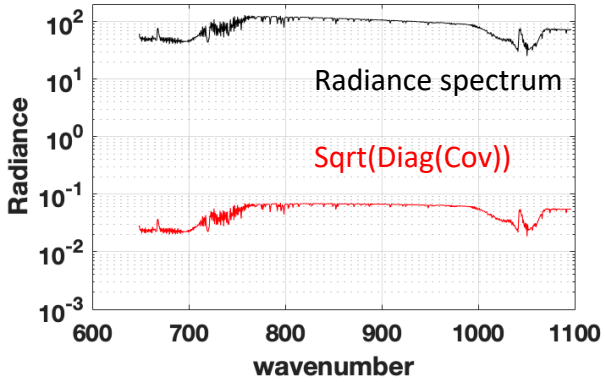

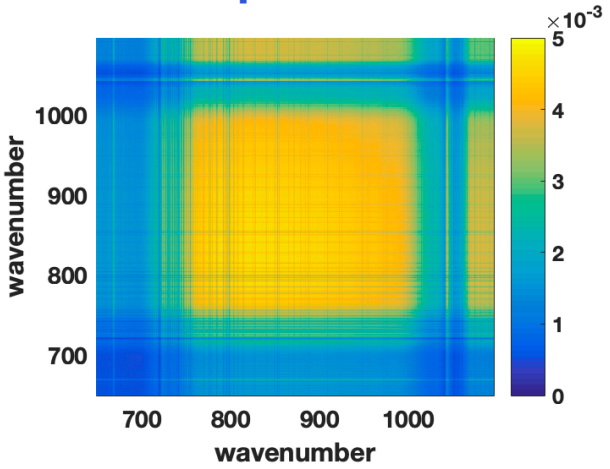

Cold cloudy scene

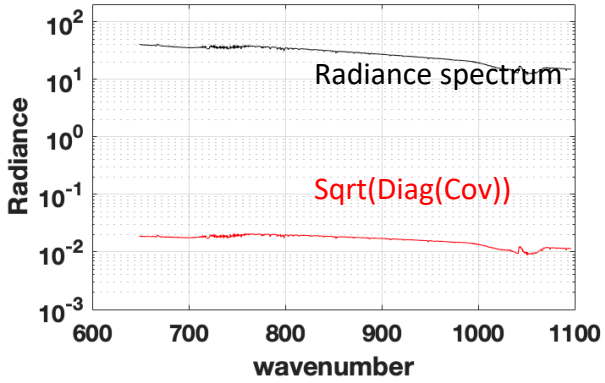

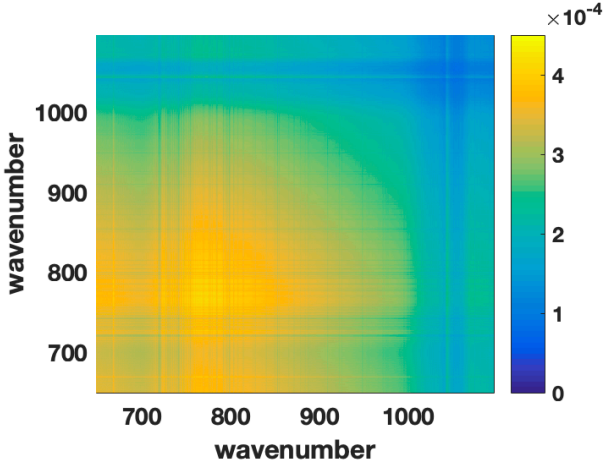

Summary and Next Steps

- CrIS noise characteristics
  - Random from footprint to footprint
  - NEDN is independent of scene; convert to NEDT at scene T if needed
  - NEDN level is FOV dependent with a few significant outliers
  - Self-apodization corrections increase NEDN and introduces noise correlation between channels, with dependencies on FOV position and channel frequency.
  - Hamming apodization reduces NEDN and further alters the spectral correlation among neighboring channels
  - Results are consistent with Han et al., and covariance matrices of various flavors are available for testing.
- CrIS calibration uncertainties
  - Generally small and stable, but scene dependent (not a stagnant “bias” in radiance or Tb) and highly spectrally correlated, and spatially correlated to the extent that adjacent scenes are spatially correlated
- Next step: Estimate covariance from “everything else”. i.e.

$$\sigma_{O\text{-}B}^2 = \sigma_{Noise}^2 + \sigma_{Cal}^2 + [\ \sigma_{RT}^2 + \sigma_{AtmState}^2 + \ldots\ ]$$